



HAL
open science

Second Generation of Near-Infrared Cyanine-Based Photocatalysts for Faster Organic Transformations

Nicolas Sellet, Leo Clement-Comoy, Mourad Elhabiri, Morgan Cormier,
Jean-philippe Goddard

► **To cite this version:**

Nicolas Sellet, Leo Clement-Comoy, Mourad Elhabiri, Morgan Cormier, Jean-philippe Goddard. Second Generation of Near-Infrared Cyanine-Based Photocatalysts for Faster Organic Transformations. Chemistry - A European Journal, 2023, 10.1002/chem.202302353 . hal-04304178

HAL Id: hal-04304178

<https://uha.hal.science/hal-04304178>

Submitted on 24 Nov 2023

HAL is a multi-disciplinary open access archive for the deposit and dissemination of scientific research documents, whether they are published or not. The documents may come from teaching and research institutions in France or abroad, or from public or private research centers.

L'archive ouverte pluridisciplinaire **HAL**, est destinée au dépôt et à la diffusion de documents scientifiques de niveau recherche, publiés ou non, émanant des établissements d'enseignement et de recherche français ou étrangers, des laboratoires publics ou privés.

Second Generation of Near-Infrared Cyanine-Based Photocatalysts for Faster Organic Transformations

Nicolas Sellet,^a Leo Clement--Comoy,^a Mourad Elhabiri,^b Morgan Cormier,^{*a} and Jean-Philippe Goddard^{*a}

^a Laboratoire d'Innovation Moléculaire et Applications (LIMA), UMR 7042, Université de Haute-Alsace (UHA), Université de Strasbourg, CNRS, 68100, Mulhouse, FRANCE

^b Laboratoire d'Innovation Moléculaire et Applications (LIMA), Bioorganic and MUMR 7042, Université de Strasbourg, Université de Haute-Alsace (UHA), CNRS, Team Bio(IN)organic and Medicinal Chemistry, European School of Chemistry, Polymers and Materials (ECPM), 67087, Strasbourg, FRANCE

Abstract: A second generation of cyanine-based near-infrared photocatalysts has been developed to accelerate organic transformations. Cyanines were prepared and fully characterized prior to evaluation of their photocatalytic activities. Catalyst efficiency was determined using two model oxidation and reduction reactions. For the aza-Henry reaction, cyanines bearing an amino group on the heptamethine chain allowed to obtain the best results. For trifluoromethylation, the stability of the photocatalyst was found to be the key parameter for efficient and rapid conversion.

Introduction

In the last decades, photoredox synthetic methods have emerged as a reliable tool to control the reactivity and selectivity of radical intermediates.¹ Organic dyes have proven to be excellent visible light-absorbing species to perform photocatalysis: redox and/or photosensitization reactions.² In this range of irradiation, many well-known photocatalysts such as Eosin Y³ or Rose Bengal⁴ are now accessible to develop the photocatalysis in a gentler manner, compatible with aqueous media. Unfortunately, visible light irradiation displays some drawbacks such as selectivity control⁵ and poor penetration in reaction media⁶ and through biological tissues.⁷ To overcome these limitations, the use of a less energetic source of irradiation such as the near-infrared (NIR) light has been considered.^{8,9} In addition, to keep the advantages of organic dyes in synthesis, NIR light-absorbing dyes have gradually emerged as valuable and powerful photocatalysts in recent years.

We were the first to demonstrate that cyanine dyes displaying interesting photophysical properties can be considered as versatile catalysts performing photoredox catalysis and photosensitization under NIR-irradiation.¹⁰ Following this, bridged-Eosin Y was used for diazonium salt reduction under NIR light.¹¹ Recently, we reported that squaraine dyes are interesting photocatalysts showing differences in term of reactivity compared to cyanines.¹² Among these last-mentioned photocatalytic systems, cyanines correspond to the more accessible organic NIR-photocatalysts for molecular chemists. Indeed, many cyanine structures are commercially available from various suppliers. Furthermore, cyanines are currently the most versatile NIR-photocatalysts; they can perform oxidation, reduction, and photosensitization reactions. They are composed by two nitrogen-containing heterocycles (pyrrole, imidazole, thiazole, quinoline, indole, etc.) linked by a polymethine chain.¹³ These cyanine dyes are also well known in biology for their use as fluorescent probes.¹⁴ Cyanines are also being developed in medicinal chemistry as photosensitizers for photodynamic therapy.¹⁵ In the last decade, the number of examples using these dyes in polymer chemistry has increased, particularly to initiate radical and/or cationic photopolymerization.¹⁶ These applications demonstrated that their photophysical properties can be useful to generate active species like radicals or cations. Since our first reported example of photoredox catalysis based on **Cy746**, no other cyanine dye has been developed

and applied to organic synthesis. However, this first generation of cyanines based NIR-photocatalyst (**Cy746**) needs improvements, especially in terms of kinetics (Figure 1). In this work, 21 cyanines were tested in model organic reactions to find the second generation of cyanine-based NIR photocatalyst with improved kinetic parameters for both oxidative and reductive processes. Herein, the redox potentials of these cyanines were also measured, providing an important dataset of spectroscopic and physico-chemical properties.

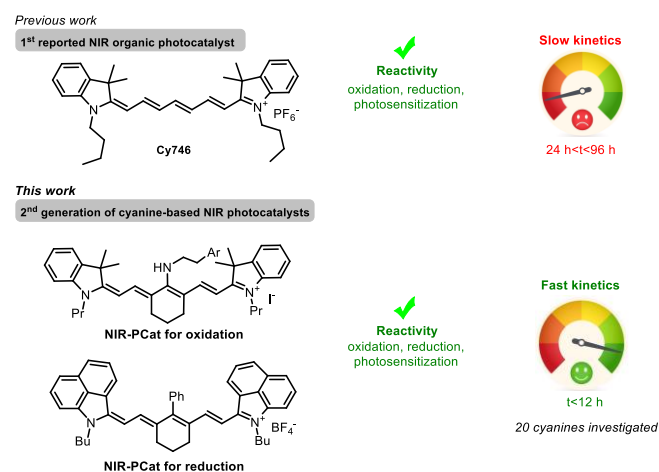
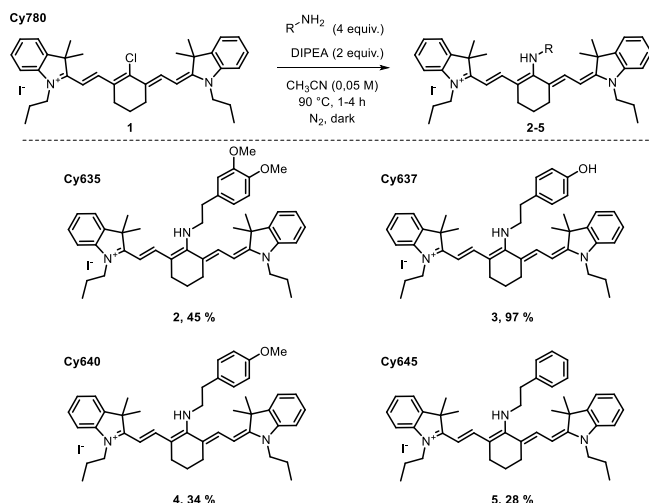


Figure 1. Cyanine scaffolds as NIR photocatalysts

Results and Discussion

While purchasing several commercial cyanine dyes, we found out that no cyanine bearing an amine donor moiety on the central position of the polymethine chain was available. In order to obtain a wider range of structures and properties we thought that these cyanine analogues might be of interest. For that purpose, a quick and straightforward synthetic approach to access this type of cyanine dyes has been developed. According to previous literature procedures, a chlorinated cyanine was derivatized.¹⁷ The examples reported in the literature are few and not fully described for this type of modification, the procedure was adapted to the targeted compounds.



Scheme 1. Derivation of Cy780

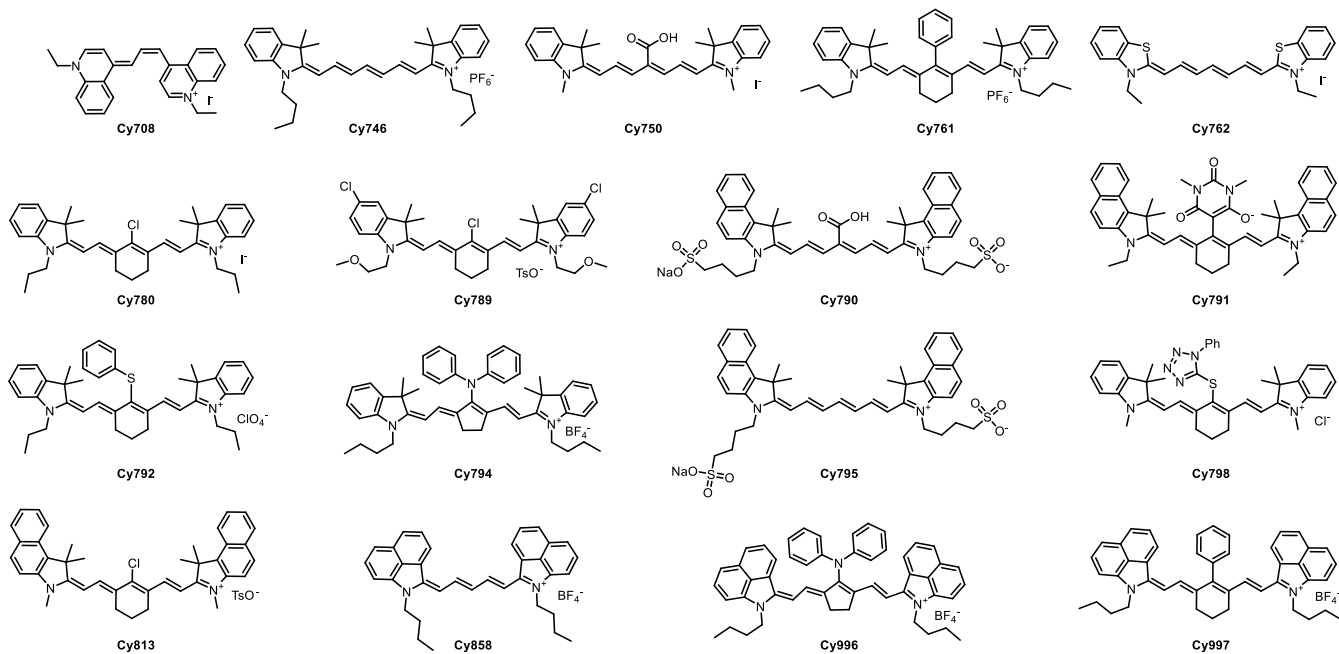
After optimization, the central chlorinated position on the polymethine chain of **Cy780** was substituted by different primary amines (Scheme 1). These amines were chosen with respect to their aromatic substitutions in order to influence the electron density and/or the solubility. To compare the photocatalytic activity of each new cyanines, phenyl, phenol, methoxyphenyl and dimethoxyphenyl moieties were selected for this study. To prevent the degradation of the cyanine dyes during the preparation, their synthesis was carried out under an inert atmosphere and in the dark. For all the reactions investigated, this optimized method provides modified cyanines with full conversion of the corresponding starting materials. **Cy637** was obtained with the best isolated yield (97%). Since the purity of the photocatalysts was crucial for the kinetic investigations, **Cy635**, **Cy640** and **Cy645** were obtained in moderate yields (28-46%) due to over purification steps. Indeed, small amounts of by-products were observed in the crude mixtures and the purifications were difficult to achieve. Furthermore, a partial degradation of the cyanine dyes was observed during the chromatographic step.

The use of cyanine dyes as photocatalysts in photoredox processes is still underestimated. The lack of reported photophysical and redox properties in literature is certainly one parameter that limits this application. To gain a better understanding of these photocatalysts, spectroscopic and redox properties were measured in DMSO on seventeen commercial cyanine dyes (Figure 2) and the four newly synthesized ones. DMSO solvent was preferred because the model oxidation and reduction reactions were performed in the same solvent. As a result, a wide range of cyanine dyes were investigated, with absorption wavelengths, oxidation and reduction potentials that cover a broad range of properties, allowing us to assess the importance of the chemical structure and the substitution pattern on the photocatalytic efficiency.

Cyclic voltammograms (CV) were recorded for all the selected cyanine dyes in DMSO with $n\text{-Bu}_4\text{PF}_6$ as supporting salt (ESI). Good agreement can be first observed between the measured data and those reported in the literature for identical or similar compounds, as illustrated for example by the values available for **Cy996** ($E_{\text{ox}} = 0.61$ V, $E_{\text{red}} = -0.25$ V), **Cy997** ($E_{\text{ox}} = 0.66$ V, $E_{\text{red}} = -0.34$ V), **Cy791** ($E_{\text{ox}} = 0.48$ V, $E_{\text{red}} = -0.97$ V)¹⁸ **Cy708** ($E_{\text{ox}} = 0.55$ V, $E_{\text{red}} = -0.86$ V)¹⁹ **Cy746** ($E_{\text{ox}} = 0.56$ V, $E_{\text{red}} = -0.63$ V).^{16a} As far as the ground state is concerned, the cyanine dyes with electro-donating substitution at the central position of the polymethine chain (**Cy635**, **Cy637**, **Cy640**,

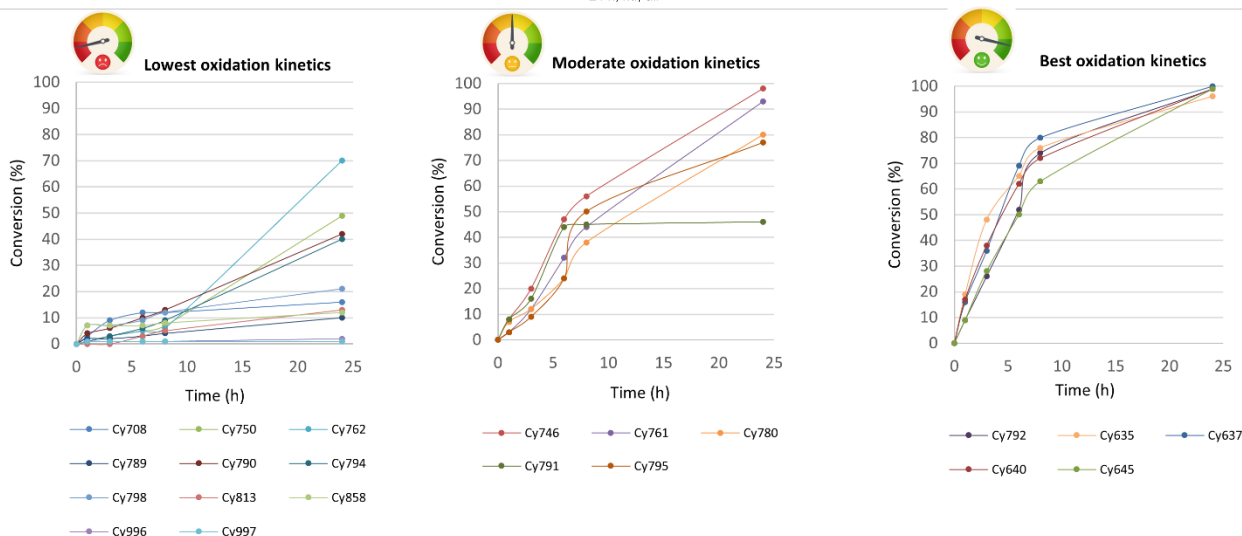
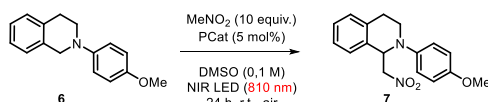
Cy645) were found to be less oxidizing with their reduction potentials being cathodically shifted with respect to that of the unsubstituted related analogue **Cy746**. The reduction peaks of the thioaryl and diphenylamine substituted cyanines (**Cy794** and **Cy792**) are slightly shifted to anodic potential comparing to **Cy746**, likely as the consequence of the aryl units. While electron delocalization could be expected for **Cy761** with respect to the unsubstituted analogue **Cy746**, a negligible influence was however observed on the reduction peak. As anticipated, with electron-withdrawing substitution at the same position (**Cy750**, **Cy780**, **Cy789**, **Cy813**), the reduction peaks were observed to be anodically shifted making these dyes more oxidizing at the ground state. The cyanine dyes with an extended conjugated system (**Cy996**, **Cy997**) both at the terminal and central positions were found to be much more oxidizing at the ground state than their respective congeners **Cy794** and **Cy761**. For example, a strong influence of this extra-conjugation (cathodic shift of ~ 400 mV) could be also observed when comparing **Cy858** to **Cy746**, **Cy996** to **Cy794** and **Cy997** to **Cy761** (Figure 2). Taken together, these first data confirmed the essential role of the substitution at the central position of the polymethine chain as well as the extra-conjugation on the reduction potential. As far as the oxidation of these cyanine dyes is concerned, the same effects as those observed for the reduction can be also used to explain the variations obtained. Although in this case the analysis is more complicated due to the presence of several oxidation peaks depending on the nature of the cyanine dye and its substitution (Figure 2). For example, the cyanines containing amine display a first oxidation signal that is cathodically shifted with respect to the analogue **Cy746**. Taken together, the ground state potentials of the oxidation and reduction processes measured for this large series of cyanine dyes are both distributed over a wide range of potentials (0.33 V $< E_{\text{ox}} < 0.88$ V and -0.24 V $< E_{\text{red}} < -0.90$ V).

With these results in hand, their excited state redox potentials E_{red}^* and E_{ox}^* were calculated by the Rehm-Weller equation using their ground state potentials and their UV-Vis absorption spectra (Figure 2).²⁰ In order to compare these data obtained for this large series of photocatalysts, two different organic transformations were carried out in oxidation and reduction. These redox photocatalytic transformations were chosen for comparison with the previous work done with **Cy746**.¹⁰ To first explore their potential in oxidation reactions, the aza-Henry reaction involving *N*-aryltetrahydroisoquinoline **6** and nitromethane was selected as a model transformation to evaluate the catalytic activity of the photocatalyst. It is important to note that the redox potential of **6** was already described in acetonitrile ($E_{\text{ox}} = 0.62$ V vs SCE).²¹ Considering the latter value as a mere estimate in DMSO and the reduction potentials measured for cyanine photocatalysts in the excited state (Figure 2), the aza-Henry reaction was first proposed to be possible (regarding a single electron transfer mechanism) with all dyes considered in this work except for **Cy791** bearing a barbiturate unit.



PCat	λ_{\max} (nm)	$E_{0,0}$ (eV)	Cy/Cy* Measured vs. Ag/AgCl		Referenced to SCE (V)		$E^*_{\text{red/ox}}$ vs SCE (V)	
			E_{ox}	E_{red}	E_{ox}	E_{red}	E^*_{ox}	E^*_{red}
Cy635	635	1.57	0.33	-0.86	0.30	-0.89	-1.27	0.68
Cy637	637	1.57	0.41	-0.82	0.38	-0.85	-1.19	0.72
Cy640	640	1.58	0.40	-0.82	0.37	-0.83	-1.21	0.75
Cy645	645	1.60	0.42	-0.82	0.39	-0.85	-1.21	0.75
Cy708	708	1.62	0.57	-0.88	0.54	-0.91	-1.08	0.71
Cy746	746	1.48	0.64	-0.65	0.61	-0.68	-0.88	0.80
Cy750	750	1.32	0.57	-0.44	0.54	-0.47	-0.78	0.85
Cy761	761	1.47	0.63	-0.69	0.60	-0.72	-0.87	0.74
Cy762	762	1.44	0.56	-0.66	0.53	-0.69	-0.92	0.75
Cy780	780	1.41	0.70	-0.54	0.67	-0.57	-0.74	0.84
Cy789	789	1.36	0.75	-0.47	0.72	-0.50	-0.65	0.86
Cy790	790	1.35	0.47	-0.47	0.44	-0.50	-0.91	0.84
Cy791	791	1.41	0.44	-0.90	0.41	-0.93	-1.00	0.48
Cy792	792	1.39	0.64	-0.56	0.61	-0.59	-0.79	0.80
Cy794	794	1.38	0.61	-0.61	0.58	-0.64	-0.80	0.74
Cy795	795	1.42	0.59	-0.68	0.56	-0.71	-0.86	0.70
Cy798	798	1.39	0.66	-0.49	0.63	-0.52	-0.77	0.87
Cy813	813	1.36	0.65	-0.56	0.62	-0.59	-0.75	0.77
Cy858	858	1.31	0.88	-0.30	0.85	-0.33	-0.46	0.97
Cy996	996	1.04	0.67	-0.24	0.64	-0.27	-0.41	0.77
Cy997	997	1.06	0.71	-0.24	0.68	-0.27	-0.38	0.79

Figure 2. Redox potentials measured for the cyanine dyes. $E_{\text{red/ox}}$ of cyanine dyes were measured by cyclic voltammetry (CV) with respect to KCl(3 M)/Ag/AgCl reference electrode and corrected vs. SCE. The solvent was DMSO, $I = 0.1$ M n-Bu₄NPF₆, $V = 200$ mV s⁻¹, and $T = 23(1)$ °C. The working electrode was a glassy carbon disk of 0.07 cm² area, and the auxiliary electrode was Pt wire.



Schema 2. Aza Henry kinetic profiles. Reactions were run on 0.1 mmol scale. Conversion rates were determined on the crude by ¹H-NMR

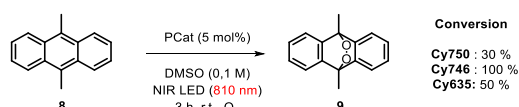
All conversion rates and kinetic profiles are reported in scheme 2, and the data obtained for **Cy746** are shown for comparison.¹⁰ The conversion profiles could be divided into three categories according to their conversion rates. The first category has the lowest rate with less than 20 % of conversion after 6h of reaction; the second is moderate, with 20% to 50 % conversion after 6h. The last category includes the best photocatalysts with conversion rates greater than 50 %. **Cy746** considered in a previous work¹⁰ can be classified as a moderate oxidant with a conversion rate slightly lower than 50 % after 6h of reaction ($E_{red}^* = 0.80$ V vs SCE in DMSO). Cyanine dyes with electron-donating groups are among the most efficient photocatalysts, with conversion rates above 50% after 6h of reaction. Close to the oxidation potential of model compound **6**, these dyes have the lowest E_{red}^* values (0.68-0.75 V). Compound **Cy792** completes this first series with however a higher E_{red}^* value of 0.80 V. The second series of photocatalysts, which can be described as moderate (conversion between 20 and 50% after 6h of reaction), includes the dyes **Cy761** ($E_{red}^* = 0.74$ V), **Cy795** ($E_{red}^* = 0.70$ V) and **Cy780** ($E_{red}^* = 0.84$ V). These dyes also lead to excellent conversions of over 80% after 24h of reaction in agreement with their reduction potential at the excited state. **Cy791** bearing a barbiturate moiety showed a close kinetic profile as **Cy746** before 6h of reaction, although its E_{red}^* value is significantly lower ($E_{red}^* = 0.48$ V). No conversion was observed after 6h, suggesting a possible degradation of **Cy791** or corresponding to its low excited state reduction potential, which theoretically prevents this reaction from occurring. With the slowest kinetics and consequently the lowest conversion rates, the excited states of cyanine dyes with an extended conjugated system (**Cy996**, **Cy997**) proved ineffective with tetrahydroisoquinoline **6**. This result is surprising given the calculated E_{red}^* of these two cyanine derivatives (0.77-0.79 V), and suggests the occurrence of other parallel processes. Although **Cy708** ($E_{red}^* = 0.71$ V), **Cy762** ($E_{red}^* = 0.75$ V), **Cy750** ($E_{red}^* = 0.85$ V), **Cy813** ($E_{red}^* = 0.77$ V) and **Cy794** ($E_{red}^* = 0.74$ V) have suitable reduction potentials for the oxidation of **6**, their reaction kinetics are relatively slow and conversion rates generally do not exceed 50% after 24h of reaction. **Cy750**, **Cy789**, **Cy790**, **Cy798** and

Cy858 are characterized by higher potentials, ranging from 0.84 to 0.97 V. With a few exceptions, cyanine dyes decorated with electron donating groups (**Cy635**, **Cy637**, **Cy640**, **Cy645**) are thus the most reactive in this model oxidation reaction, giving up to 70% conversion after 6h (more than 90% conversion after 24h). These are indeed more reactive than analogues with electron-withdrawing groups or additional aromatic groups (central or terminal), which allow greater delocalization. For example, dihydrobenzo[*cd*]indole appears to have a significant effect on the oxidation reaction, especially when comparing the conversion by **Cy761** and **Cy997**, by **Cy746** and **Cy858** or to a lesser extent by **Cy794** and **Cy996**. Taken together, these data strongly suggest other parallel processes affecting the oxidation reaction of **6** or the stability of the NIR dye. Indeed, the calculated E_{red}^* values would suggest that most of the photocatalysts would participate in this aza-Henry reaction to varying degrees depending on the gap between the excited state reduction potential of the dye and the oxidation potential of compound **6**. With the exception of dyes **Cy791** and **Cy858**, all E_{red}^* values fall within the range 0.68 V to 0.87 V, with marked effects on reaction efficiency (e.g., **Cy794** with $E_{red}^* = 0.74$ V and **Cy640** with $E_{red}^* = 0.75$ V). Comparing all the kinetic profiles, there is thus no apparent correlation between the redox potential at the excited state and the efficiency of the aza-Henry transformation.

The photo-degradation of cyanine dyes in the presence of O₂ has been investigated in the literature²² with the main degradation pathway corresponding to the cycloaddition of singlet oxygen onto the polymethine chain to generate the corresponding aldehydes. Furthermore, this lack of clear relationship can be explained by the complexity of mechanism involved in the aza-Henry reaction.²³ Indeed, direct oxidation

of tetrahydroisoquinoline **6** by the excited state photocatalyst through a SET process can take place. However, the generation of singlet oxygen can also occur, resulting, after oxidation of **6**, in the same iminium intermediate (ESI p39).

To investigate the ability of these NIR dyes to photosensitize oxygen, we selected three different cyanines with low, moderate, and high efficiencies to photocatalyze the first oxidation reaction. For this purpose, the oxidation of 9,10-dimethylantracene **8** was performed as test reaction, known to occur selectively through a $^1\text{O}_2$ mechanism (Scheme 3).²⁴ After 3h of irradiation at 810 nm, we observed a huge difference in the conversions between the selected photocatalysts, with only **Cy746** giving a complete conversion of **8** to **9**. In addition, control experiments were performed, without PCat or in the dark, and no conversions were observed. This result suggests that the cyanines do not have the same ability to convert triplet oxygen to singlet oxygen, which may have a major effect on the aza-Henry reaction.

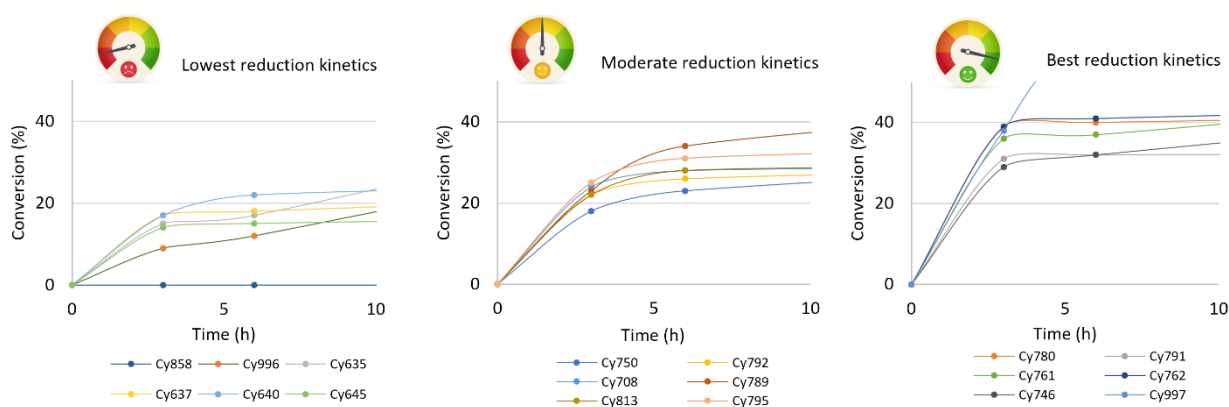
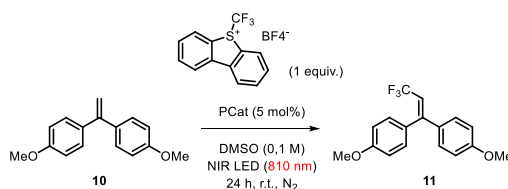


Scheme 3. Photooxidation of 9,10-dimethylantracene. Reactions were run at 0.1 mmol scale, and conversions were determined on the crude by $^1\text{H-NMR}$.

A second study was then performed to evaluate the ability of the cyanine dyes to undergo oxidation at the excited state. For this purpose, a trifluoromethylation reaction was chosen.²⁵ With respect to oxidation of compound **6**, the same kinetic rate study was performed to reveal different photoredox reactivity. Umemoto salt was the source of the trifluoromethyl radical with an E_{red} value of -0.75 V vs. Fc/Fc^+ ($E_{\text{red}} = -0.44\text{ V}$ vs. SCE) and 1,1-bis(4-methoxyphenyl)ethene¹⁰ acted as the acceptor

(Scheme 4). As before, the kinetics of the trifluoromethylation (product **11**) were classified into three categories. The least reactive class resulted in conversions of less than 20% after 3 h, the moderate class resulted in conversions of about 20% after 3h, and the best kinetic profiles corresponded to conversions of more than 30% (Scheme 4). With the exception of compounds **Cy858** ($E_{\text{ox}}^* = -0.46\text{ V}$), **Cy996** ($E_{\text{ox}}^* = -0.41\text{ V}$) and **Cy997** ($E_{\text{ox}}^* = -0.38\text{ V}$), all reactions are predicted to be possible, but these three E_{ox}^* are close to the required potential for this transformation. The synthesized cyanines dyes (**Cy635**, $E_{\text{ox}}^* = -1.27\text{ V}$; **Cy637**, $E_{\text{ox}}^* = -1.19\text{ V}$, **Cy640**, $E_{\text{ox}}^* = -1.21\text{ V}$ and **Cy645**, $E_{\text{ox}}^* = -1.21\text{ V}$) bearing secondary amines at the central position of the polymethine chain were shown to be much more reducing than the commercial cyanines at their excited states. In general, the least reducing compounds in the excited state are cyanine dyes with extended terminal conjugation as shown by the comparison of **Cy996** ($E_{\text{ox}}^* = -0.41\text{ V}$) with **Cy794** ($E_{\text{ox}}^* = -0.80\text{ V}$), **Cy997** ($E_{\text{ox}}^* = -0.38\text{ V}$) with **Cy761** ($E_{\text{ox}}^* = -0.87\text{ V}$), or **Cy858** ($E_{\text{ox}}^* = -0.46\text{ V}$) with **Cy746** ($E_{\text{ox}}^* = -0.88\text{ V}$).

For all the kinetic profiles investigated, in general, a plateau is reached after 4h of reaction and no further conversion is observed thereafter. This result suggests a possible degradation of the cyanine scaffold during the reduction reaction investigated. We thus evaluated this hypothesis by isolating **Cy746** after reaction with the Umemoto salt to see if the CF_3 radical generated could add to the polymethine chain, which could, for example, lead to inhibition of the photocatalytic system. Numerous new products were indeed observed by $^{19}\text{F-NMR}$ whose structures could not be fully determined, which could correspond to a non-selective trifluoromethylation reaction of cyanine (ESI p37).

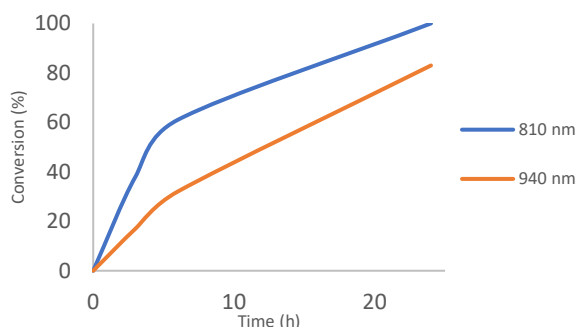


Scheme 4. Trifluoromethylation kinetic profiles. Reactions were run on 0.1 mmol scale, conversions were determined on the crude by $^1\text{H-NMR}$.

Although the newly synthesized cyanines show the best calculated E_{ox}^* around -1.20 V (compared to SCE in DMSO), the conversion rates were very low. Interestingly, only **Cy997** achieved full conversion to the desired product after 24h of reaction. In this case, we did not observe the same plateau on

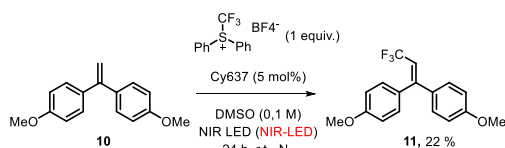
the kinetic profile, strongly suggesting that the stability of this photocatalyst is much higher in the presence of the trifluoromethyl radical. To complement and take this result a step further, we studied the photocatalytic activity of **Cy997** with a lower irradiation energy source, at 940 nm (Scheme 5).

The reaction kinetics proved to be slower, with a conversion rate of about 80% achieved after 24h of reaction. This result is a rare example of NIR-photocatalysis for an organic conversion beyond 900 nm.



Scheme 5. Trifluoromethylation of **10** using **Cy997** as the NIR-photocatalyst and conditions of scheme 4. Reactions were run on 0.1 mmol scale, conversions were determined on the crude by $^1\text{H-NMR}$

We then tried the more challenging Yagupolskii-Umemoto salt reduction ($E_{\text{red}} = -1.05 \text{ V vs. Fc/Fc}^+$, $E_{\text{red}} = -0.74 \text{ V vs. SCE}$) with all the cyanines considered in this work.²³ The best result was obtained with the most reducing cyanine, **Cy637**, which gave only 22% conversion after 24h of irradiation (Scheme 6). For the other photocatalysts tested, no trace of reduction was observed.



Scheme 6. Reduction of Yagupolskii-Umemoto's reagent.

Conclusion

In this study, we prepared four new cyanines and provided photophysical and electrochemical data on a large series of 21 NIR-absorbing photocatalysts. Using the Rehm-Weller approach, these spectroscopic and redox data allowed us to evaluate the oxidation and reduction potentials in the excited state of these cyanine dyes. This second generation of cyanine-based NIR photocatalysts was then investigated for the oxidation of tetrahydroisoquinoline **6**. Cyanines with an amino group on the heptamethine chain were found to be the best photocatalysts for accelerating the aza-Henry reaction. Considering the different kinetics obtained and the test reactions with 9,10-dimethylantracene, cooperative mechanisms involving SET and $^1\text{O}_2$ generation are most likely responsible for the formation of the product **7**. The parallel study focused on the reduction of Umemoto salts for the trifluoromethylation of alkenes. The data obtained not only demonstrated the instability of most photocatalysts under these experimental conditions, but also highlighted **Cy997** as the best NIR photocatalyst for carrying out this reaction. In fact, this cyanine dye is more stable under these reducing conditions, allowing efficient conversion to the trifluoromethylated product even under irradiation at lower energy at 940 nm. Further studies will be carried out in the future to deepen our understanding of cyanine-based photocatalytic systems, including DFT calculations and more in-depth photophysical studies.

Experimental Section

General procedure for the synthesis of cyanine dyes

Cyanine dyes were synthesized following a modified literature procedure¹⁷: **Cy780 (1)** (300 mg, 0.43 mmol, 1 equiv.) and the amine (1.71 mmol, 4 equiv.) were introduced into a 50 mL flask. The flask was placed under an inert atmosphere with nitrogen. Then distilled acetonitrile (18 mL) and DIPEA (141 μL , 0.85 mmol, 2 equiv.) were successively added at room temperature. The reaction media was then heated to 90 $^\circ\text{C}$ for 1 to 4h in the dark before cooling and treatment with 1 N HCl solution (60 mL). The aqueous phase was extracted 3 times with 30 mL ethyl acetate. The collected organic phases were washed with a saturated sodium chloride solution and dried over MgSO_4 . The solvent was evaporated under reduced pressure and the crude product was purified by alumina column (dichloromethane/ methanol: 98/2) to give corresponding cyanine dyes as solids.

Synthesis of 2-((E)-2-((E)-2-((3,4-dimethoxyphenethyl)amino)-3-(2-((E)-3,3-dimethyl-1-propylindolin-2-ylidene)ethylidene)cyclohex-1-en-1-yl)vinyl)-3,3-dimethyl-1-propyl-3H-indol-1-ium iodide (2)

Cy635 was obtained following the general procedure, after 2h of reaction in 45 % isolated yield as a dark blue solid. $^1\text{H NMR}$ (400 MHz, CDCl_3) δ 10.56 (brs, 1H), 7.70 (d, $J = 12.2 \text{ Hz}$, 2H), 7.23-7.19 (m, 4 H), 6.99 (t, $J = 7.3 \text{ Hz}$, 2H), 6.82 (s, 1 H), 6.77 (d, $J = 7.7 \text{ Hz}$, 2H), 6.71 (s, 2H), 5.47 (d, $J = 12.7 \text{ Hz}$, 2H), 4.23-4.14 (m, 2H), 3.80 (s, 3H), 3.79 (s, 3H), 3.69 (t, $J = 6.7 \text{ Hz}$, 4H), 3.28 (t, $J = 6.6 \text{ Hz}$, 2H), 2.29 (t, $J = 6.1 \text{ Hz}$, 4H), 1.87-1.66 (m, 18H), 1.00 (t, $J = 7.5 \text{ Hz}$, 6H). $^{13}\text{C NMR}$ (126 MHz, CDCl_3) δ 171.6, 166.3, 148.7, 147.4, 143.5, 140.4, 136.5, 131.7, 127.9, 122.1, 122.0, 121.0, 120.3, 112.9, 11.2, 107.9, 93.3, 56.1, 56.0, 51.2, 47.6, 44.5, 36.8, 29.0, 25.6, 21.2, 20.0, 11.8. **FT-IR** (v/cm^{-1}): 2961, 2926, 2871, 2251, 2179, 1724, 1673, 1514, 1100, 917, 798, 714. **HRMS (ESI+)** m/z : $[\text{M}]^+$ 684.4524 calcd for $\text{C}_{46}\text{H}_{58}\text{N}_3\text{O}_2$, found 684.4554.

Synthesis of 2-((E)-2-((E)-3-(2-((E)-3,3-dimethyl-1-propylindolin-2-ylidene)ethylidene)-2-((4-hydroxyphenethyl)amino)cyclohex-1-en-1-yl)vinyl)-3,3-dimethyl-1-propyl-3H-indol-1-ium iodide (3)

Cy637 was obtained following the general procedure after 1h of reaction in 97 % isolated yield as a dark blue solid. $^1\text{H NMR}$ (400 MHz, CDCl_3) δ 8.97 (brs, 1H), 8.63 (brs, 1H), 7.55 (d, $J = 12.6 \text{ Hz}$, 2H), 7.23-7.17 (m, 4H), 7.02-6.90 (m, 6H), 6.78 (d, $J = 7.9 \text{ Hz}$, 2H), 5.50 (d, $J = 12.7 \text{ Hz}$, 2H), 4.04-4.01 (m, 2H), 3.73-3.67 (m, 4H), 3.05 (t, $J = 6.3 \text{ Hz}$, 2H), 2.31 (t, $J = 6.3 \text{ Hz}$, 4H), 1.78-1.70 (m, 4 H), 1.63-1.52 (m, 14H), 0.96 (t, $J = 7.5 \text{ Hz}$, 6H). $^{13}\text{C NMR}$ (126 MHz, CDCl_3) δ 170.2, 166.8, 156.6, 143.3, 140.2, 136.8, 129.4, 127.9, 127.6, 122.4, 122.2, 116.3, 108.2, 94.0, 51.0, 47.6, 44.6, 28.9, 25.5, 21.1, 20.0, 11.8. **FT-IR** (v/cm^{-1}): 3053, 2962, 2927, 2871, 1513, 1110, 915, 740, 714. **HRMS (ESI+)** m/z : $[\text{M}]^+$ 640.4261 calcd for $\text{C}_{44}\text{H}_{54}\text{N}_3\text{O}$, found 640.4254.

Synthesis of 2-((E)-2-((E)-3-(2-((E)-3,3-dimethyl-1-propylindolin-2-ylidene)ethylidene)-2-((4-methoxyphenethyl)amino)cyclohex-1-en-1-yl)vinyl)-3,3-dimethyl-1-propyl-3H-indol-1-ium iodide (4)

Cy640 was obtained following the general procedure after 3.5h of reaction in 34 % isolated yield as a dark blue solid. ^1H

NMR (400 MHz, CDCl₃) δ 9.66 (brs, 1H), 7.67 (d, *J* = 12.6 Hz, 2H), 7.23-7.20 (m, 4H), 7.15 (d, *J* = 8.5 Hz 2H), 7.00 (t, *J* = 7.3 Hz, 2 H), 6.80-6.75 (m, 4H), 5.51 (d, *J* = 12.6 Hz, 2H), 4.17-4.11 (m, 2H), 3.78-3.67 (m, 7H), 3.25 (t, *J* = 6.4 Hz, 2H), 2.33 (t, *J* = 6.3 Hz, 4H), 1.82-1.57 (m, 18H), 1.00 (t, *J* = 7.4 Hz, 6H). **¹³C NMR** (126 MHz, CDCl₃) δ 171.5, 166.3, 158.1, 143.6, 140.5, 136.7, 131.1, 130.2, 127.9, 122.2, 122.1, 120.3, 113.8, 107.9, 93.4, 55.4, 53.6, 51.1, 47.6, 44.6, 36.2, 29.1, 25.6, 21.3, 20.1, 11.9. **FT-IR (ν/cm⁻¹):** 2960, 2925, 2870, 2115, 1674, 1612, 1511, 1099, 916, 798. **HRMS (ESI+)** *m/z*: [M]⁺ 654.4418 calcd for C₄₅H₅₆N₃O, found 654.4406.

Synthesis of 2-((E)-2-((E)-3-(2-((E)-3,3-dimethyl-1-propylindolin-2-ylidene)ethylidene)-2-(phenethylamino)cyclohex-1-en-1-yl)vinyl)-3,3-dimethyl-1-propyl-3H-indol-1-ium iodide (5)

Cy645 was obtained following the general procedure after 4h of reaction in 28 % isolated yield as a dark blue solid. **¹H NMR** (400 MHz, CDCl₃) δ 9.82 (brs, 1H), 7.69 (d, *J* = 12.4 Hz, 2H), 7.25-7.20 (m, 8H), 7.16-7.12 (m, 1H), 7.01 (t, *J* = 6.9 Hz, 2H), 6.80 (d, *J* = 7.9 Hz, 2H), 5.51 (d, *J* = 12.7 Hz, 2H), 4.23-4.18 (m, 2H), 3.80-3.64 (m, 4H), 3.34 (t, *J* = 6.7 Hz, 2H), 2.32 (t, *J* = 6.3 Hz, 4H), 1.83-1.74 (m, 4H), 1.68 (brs, 12H), 1.59-1.53 (m, 2H), 1.01 (t, *J* = 7.4 Hz, 6H). **¹³C NMR** (126 MHz, CDCl₃) δ 171.5, 166.3, 143.5, 140.5, 139.0, 136.7, 129.3, 128.3, 127.9, 126.2, 122.1, 122.0, 120.3, 107.9, 93.4, 50.9, 47.6, 44.6, 37.1, 29.0, 22.5, 21.3, 20.0, 11.9. **FT-IR (ν/cm⁻¹):** 2961, 2926, 2870, 2115, 1518, 1100, 916, 713. **HRMS (ESI+)** *m/z*: [M]⁺ 624.4312 calcd for C₄₄H₅₄N₃, found 624.4307.

Synthesis of 2-(4-methoxyphenyl)-1-(nitromethyl)-1,2,3,4-tetrahydroisoquinoline (7)

2-(4-methoxyphenyl)-1,2,3,4-tetrahydroisoquinoline (0.13 mmol, 1 equiv.) (**6**), freshly distilled nitromethane (1.3 mmol, 10 equiv.), PCat (66 μmol, 5 mol%) and DMSO-d₆ (1.3 mL) were charged in a reaction glass tube with magnetic stirring bar. The reaction mixture was stirred under air atmosphere and near infrared LED (810 nm) irradiation (2-3 cm away from the light source) at room temperature for 24h. The conversion in **7** was given by ¹H NMR spectrometry. The data correspond to the isolated product **7**. **¹H NMR** (400 MHz, CDCl₃) δ 7.29–7.16 (m, 4H), 6.95 (dt, *J* = 9.1, 3.5 Hz, 2H), 6.85 (dt, *J* = 9.1, 3.5 Hz, 2H), 5.43 (dd, *J* = 8.4, 5.9 Hz, 1H), 4.83 (dd, *J* = 11.9, 8.7 Hz, 1H), 4.58 (dd, *J* = 11.9, 5.9 Hz, 1H), 3.77 (s, 3H), 3.64–3.54 (m, 2H), 3.04 (m, 1H), 2.72 (dt, *J* = 16.6, 3.9 Hz, 1H). **¹³C NMR** (126 MHz, CDCl₃) δ 154.0, 143.1, 135.5, 132.9, 129.5, 127.9, 127.0, 126.6, 118.8 (2C), 114.7 (2C), 78.9, 58.9, 55.6, 43.1, 25.8.

Synthesis of 9,10-dimethyl-9,10-dihydro-9,10-epidioxyanthracene (9)

9,10-dimethylantracene (0,1 mmol, 1 equiv.) (**8**) and PCat (5 μmol, 5 mol%) were charged in a Schlenk tube with magnetic stirring bar. The reaction media was degassed 3 times and refill with O₂, then O₂ charged DMSO-d₆ (1 mL) was added. The reaction was then stirred under O₂ atmosphere and near infrared LED (810 nm or 940 nm) irradiation (2-3 cm away from the light source) at room temperature for 24h. The conversion in **9** was given by ¹H NMR spectrometry and correspond to the literature²⁴. **¹H NMR** (500 MHz, CDCl₃) δ 7.42-7.39 (m, 4H), 7.30-7.26 (m, 4H), 2.16 (s, 6H). **¹³C NMR** (126 MHz, CDCl₃) δ 140.9, 127.5, 120.8, 79.7, 13.9.

Synthesis of 4,4'-(3,3,3-trifluoroprop-1-ene-1,1-diyl)bis(methoxybenzene) (11)

1,1-bis(4-methoxyphenyl)ethene (**10**) (0,1 mmol, 1 equiv.), PCat (0.005 mmol, 5 mol%) were charged in a reaction glass tube with magnetic stirring bar. The reaction media was degassed 3 times and refill with N₂, then degassed DMSO-d₆ (1 mL) by freeze pump thaw technique was added. The reaction was then stirred under N₂ atmosphere and near infrared LED (810 nm) irradiation (2-3 cm away from the light source) at room temperature for 24h. The conversion in **11** was given by ¹H NMR spectrometry and correspond to the literature.²⁵ **¹H NMR** (400 MHz, DMSO-d₆) δ 7.21 (m, 2H), 7.11 (m, 2H), 7.00 (m, 2H), 6.92 (m, 2H), 6.35 (q, *J* = 17.4, 8.8 Hz, 1H), 3.80 (s, 3H), 3.77 (s, 3H).

Acknowledgements

The authors thank UHA (University of Haute-Alsace) for providing facilities and funding.

Conflict of Interest

The authors declare no conflict of interest.

Data Availability Statement

The data that support the findings of this study are available in the supplementary material of this article.

Keywords: Near-infrared • Photocatalysis • Photosensitization • Cyanine • Redox potentials

- (1) (a) L. Candish, K.D. Collins, G. C. Cook, J. J. Douglas, A. Gomez-Suarez, A. Jolit, S. Keess, *Chem. Rev.* **2022**, *122*, 2907-2980. (b) J. D. Bell, J. A. Murphy, *Chem. Soc. Rev.* **2021**, *50*, 9540–9685. (c) R. C. McAtee, E. J. McClain, C. R. J. Stephenson, *Trends Chem.* **2019**, *1*, 111-125.
- (2) N. A. Romero, D. A. Nicewicz, *Chem. Rev.* **2016**, *116*, 10075–10166.
- (3) D. Prasad Hari, B. König, *Chem. Commun.* **2014**, *50*, 6688-6699.
- (4) S. Sharma, A. Sharma, *Org. Biomol. Chem.* **2019**, *17*, 4384-4405.
- (5) A. Bartling, A. Eisenhofer, B. König, R. M. Gschwind, *J. Am. Chem. Soc.* **2016**, *138*(36), 11860-11871.
- (6) A. H. Bonardi, T. M. Grant, G. Noirbent, D. Gignes, B. H. Lessard, J.-P. Fouassier, J. Lalevee, *J. Macromolecules* **2018**, *51*, 1314–1324.
- (7) A. M. Smith, M. C. Mancini, S. Nie, *Nat. Nanotechnol.* **2009**, *4*, 710-711.
- (8) Review about the NIR-photocatalysis: N. Sellet, M. Cormier, J.-P. Goddard, *Org. Chem. Front.* **2021**, *8*, 6783-6790.
- (9) (a) C. Grundke, R. C. Silva, W. R. Kitzmann, K. Heinze, K. T. de Oliveira, T. Opatz, *J. Org. Chem.* **2022**, *87*, 8630-5642. (b) I. M. Ogbu, D. M. Bassani, F. Robert, Y. Landais, *Chem. Commun.* **2022**, *58*, 8802-8805. (c) Y. Katsurayama, Y. Ikabata, H. Maeda, M. Segi, H. Nakai, T. Furuyama, *Chem. Eur. J.* **2022**, *28*, e2021032. (d) B. D. Ravetz, N. E. S. Tay, C. L. Joe, M. Sezen-Edmonds, M. A. Schmidt, Y. Tan, J. M. Janey, M. D. Eastgate, T. Rovis, *ACS. Cent. Sci.* **2020**, *6*, 2053-2059. (e) B. D. Ravetz, A. B. Pun, E. M. Churchill, D. N. Congreve, T. Rovis, L. M. Campos, *Nature* **2019**, *565*, 343-346.
- (10) A. R. Obah Kosso, N. Sellet, A. Baralle, M. Cormier, J.-P. Goddard, *Chem. Sci.* **2021**, *12*, 6964-6968.
- (11) M. Tanioka, A. Kuromiya, R. Ueda, T. Obata, A. Muranaka, M. Uchiyama, S. Kamino, *Chem. Commun.* **2022**, *58*, 7825-7828.
- (12) N. Sellet, M. Sebbat, M. Elhabiri, M. Cormier, J.-P. Goddard, *Chem. Commun.* **2022**, *58*, 13759-13762.
- (13) K. Colas, S. Doloczkí, M. P. Urrutia, C. Dyrager, *Eur. J. Org. Chem.* **2021**, *15*, 2133-2144.
- (14) W. Sun, S. Guo, C. Hu, J. Fan, X. Peng, *Chem. Rev.* **2016**, *116*, 7768-7817.
- (15) N. Lange, W. Szlasa, J. Saczko, A. Chwilkowska, *Pharmaceutics* **2021**, *13*, 818.
- (16)(a) Q. Wang, S. Popov, A. Feilen, V. Strehmel, B. Strehmel, *Angew. Chem., Int. Ed.* **2021**, *60*(51), 26855-26865. (b) Y. Pang, A. Shirashi, D. Keil, S. Popov, V. Strehmel, H. Jiao, J. S. Gutmann, Y. Zhou, B. Strehmel, *Angew. Chem., Int. Ed.* **2021**, *60*, 1465-1473. (c) H. Mokbel, G. Noirbent, D. Gignes, F. Dumur, J. Lalevee, *Beilstein J. Org. Chem.* **2021**, *17*, 2067-2076.

- (17) A. Samanta, R. Vendrell, R. Das, Y.-T. Chang, *Chem. Commun.* **2010**, 46, 7406-7408.
- (18) C. Schmitz, A. Halbhuber, D. Keil, B. Strehmel, *Prog. Org. Coat.* **2016**, 100, 32-46.
- (19) J. R. Lenhard, B. R. Hein, A. A. Muentner, *J. Phys. Chem.* **1993**, 97, 8269-8280.
- (20) L. Buzzetti, G. E. M. Crisenza, P. Melchiorre, *Angew. Chem., Int. Ed.* **2019**, 58, 3730-3747.
- (21) D. Prasad, B. König, *Org. Lett.* **2011**, 13, 15, 3852-3855.
- (22) S. Yang, H. Tian, H. Xiao, X. Shang, X. Gong, S. Yao, K. Chen, *Dyes and Pigments* **2001**, 49, 93-101.
- (23) J. L. Clark, J. E. Hill, I. D. Rettig, J. J. Beres, R. Ziniuk, T. Y. Ohulchanskyy, T. M. McCormick, M. R. Detty, *Organometallics* **2019**, 38, 2431-2442.
- (24) J. M. Carney, R. J. Hammer, M. Hulce, C. M. Lomas, D. Miyashiro, *Synthesis* **2012**, 44, 2560-2566.
- (25) T. Koike, M. Akita, *Acc. Chem. Res.* **2016**, 49, 1937-1945.

